Transient Electrostatic Fields and Related Energetic Proton Generation with a Plasma Fiber

Z. L. Chen,[1,*] G. R. Kumar,[1,†] Z. M. Sheng,[2] T. Matsuoka,[1] Y. Sentoku,[3] M. Tampo,[1] K. A. Tanaka,[1,4] T. Tsutsumi,[4] T. Yabuuchi,[4] and R. Kodama[1,4]

[1]*Institute of Laser Engineering, Osaka University, 2-6 Yamada-oka, Suita, Osaka 565-0871, Japan*
[2]*Beijing National Laboratory for Condensed Matter Physics, Institute of Physics, CAS, Beijing 100080, China*
[3]*Department of Physics, University of Nevada, 5625 Fox Avenue, Reno, Nevada 89506, USA*
[4]*Graduate School of Engineering, Osaka University, 2-6 Yamada-oka, Suita, Osaka 565-0871, Japan*

(Received 25 April 2005; published 3 March 2006)

We observe a hollow structure and a fine ring in the proton images from a petawatt scale laser interaction with a "cone-fiber" target. The protons related to the hollow structure are accelerated from the cone-tip surface and deflected later by a radial electric field surrounding the fiber. Those associated with the fine ring are accelerated from the fiber surface by this radial electric field. This field is found to decay exponentially within 3 ps from about 5×10^{12} V/m. Two-dimensional particle-in-cell simulations produce similar proton angular distributions.

DOI: 10.1103/PhysRevLett.96.084802 PACS numbers: 41.85.Ja, 52.40.Mj, 52.57.Kk

High-intensity femtosecond-laser interaction with matter can create plasmas that are extremely energetic and simultaneously dense [1,2]. An exciting outcome of such interaction is the production of ultrashort bursts of charged particles at MeV energies, fueling prospects for novel accelerators [3] and other related applications, such as fast ignition fusion [1,4], radiography [5], cancer therapy, etc. Protons, which have been produced with energies as high as few tens of MeV with a petawatt (PW) scale laser, are attracting particular attention [6]. Their generation at the back of a thin irradiated solid target has been modeled by the target normal sheath acceleration (TNSA) mechanism [7]. Such proton beams can be focused and used to heat compressed fusion targets as well as perform radiography of such targets [8]. Their transport, crucially affected by electric and magnetic fields in plasmas, is now established as a powerful diagnostic tool to understand the electric field formation responsible for charged particle acceleration [8].

Recently, we demonstrated guiding and collimation of a high current of MeV electrons in a carbon fiber, in a manner akin to photon transport in an optical fiber [9]. This is explained to occur by (1) the rapid heating of the carbon fiber into a plasma fiber, (2) the conduction of the fast electrons through this "plasma fiber," and (3) the guiding of these electrons by the magnetic and electric fields induced at the fiber edge by their own transport. The details of these fields have not been fully clarified yet in experiments.

In this letter, we report an experimental investigation of the transient electric field generated around a plasma fiber. We detect this field using the energetic (MeV) protons generated in a "cone-fiber" target. The MeV proton angular distribution, related to the radial electric field around the fiber, exhibits a unique feature—a hollow structure around the fiber axis and a fine ring perpendicular to the fiber axis. The experimental observation has been supported by two-dimensional particle-in-cell (PIC) simulations. The role of the radial electric field in guiding MeV electrons through the plasma fiber has been pointed out.

Experiments were performed using the PW scale laser [10] at the Institute of Laser Engineering, Osaka University. The 1.06 μm, 0.75 ps horizontally polarized 240 terawatt (TW) laser pulse with an energy of 180 J (40% of its total energy on target) was focused by an off-axis parabolic mirror ($f/7$) into a 20×50 μm^2 elliptical spot on the target. The corresponding peak laser intensity reaches 10^{19} W cm^{-2}.

We used two types of cone-fiber targets (Fig. 1, left), one with a solid carbon fiber assembled to the tip disk of a reentrant cone along its axis, called the "straight-fiber cone" in the following (black solid line in Fig. 1), and another with the solid carbon fiber assembled at an angle of 15°, called the "tilted-fiber cone" (white dashed line in Fig. 1). The reentrant cone [11] was made by assembling a gold disk of 7 μm thick and 30 μm in diameter at the tip of a 900 μm long and 20 μm thick gold reentrant-cone wall with an open angle of 30°. It was irradiated normally at its disk by the laser along the cone axis. The carbon fiber was 5 μm in diameter and 1 mm long, extending along the forward laser direction, with one end sticking to the center of the tip disk of the reentrant cone.

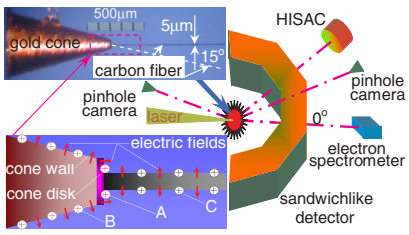

FIG. 1 (color online). Experimental configuration. An electron spectrometer is put exactly in the forward laser direction to measure the electron spectrum. A high speed sampling camera is used to observe the optical emissions from the target. Two pinhole cameras monitor the x-ray emissions from the target.

A sandwichlike detector (Fig. 1, right) was placed 30 mm away from the target to measure the energy resolved angular distribution of electrons and protons in the forward laser direction. This detector consisted of multiple layers of radiochromic films (RCFs), CR-39 sheets, and imaging plates [11]. It also used a 10 μm thick Al foil at the front side to stop the target debris and energetic heavy ions, allowing only hard x rays, energetic electrons, and protons to reach the detector. The data measured by RCFs and CR-39 sheets allow one to distinguish the protons (in the range 0.8–15.1 MeV) from other signals and to obtain energy resolved proton angular distributions.

Figure 2 shows the proton angular distribution, where a hollow structure and an intense fine ring are found in addition to the general feature in the reentrant-cone target. In the latter case two proton jets are emitted [11]—one with a direction normal to the disk [around $(0°, 0°)$] and another normal to the cone wall [around $(75°, 0°)$]. The hollow region, indicating absence of protons, is always located around the fiber axis. Its center changes from approximately $(0°, 0°)$ in the straight-fiber-cone case [Figs. 2(a) and 2(c)] to $(0°, -15°)$ in the tilted-fiber-cone case [Fig. 2(b)]. As the proton energy increases, the open angle of the hollow structure changes (see inset in Fig. 3) from approximately 40°, 60°, and 80° to 100°. The fine ring, with an intensity approximately one magnitude higher than those in other directions, is located approximately 80° to the fiber axis, indicating a beam of MeV protons with an extremely narrow angular spread in the direction perpendicular to the fiber axis.

The hollow structure and the fine ring in the proton angular distributions can be explained as arising from the induced transient electrostatic fields (see Fig. 1, bottom left) at the target-vacuum interfaces caused by MeV electrons transporting through the cone-fiber target. Protons are emitted through the TNSA mechanism: those closely outside the hollow portion in Fig. 2 are from the disk rear surface outside the cone-fiber connection region, while those forming the fine ring are from the fiber surface. The physical processes can be described as follows. First, when the generated MeV electrons move to the rear surfaces of the cone target, electrostatic fields normal to its surfaces are created. These electric fields then accelerates protons in two directions: the normal of the cone wall and the normal of the disk, resulting in such a proton emission feature as in the simple reentrant-cone target [11]—two proton jets [labeled as proton groups B and A (see Fig. 1, bottom left)]. Next, some energetic electrons in the central region move into the fiber, heat it, and turn it into plasma with a high conductivity, and then propagate through this plasma channel. A new electric field is thus induced in the radial direction on the fiber surface. The plasma fiber, in conjunction with this electric field, guides the main part of the electron beam, in a manner akin to that of light guiding in an optical fiber [8]. Meanwhile, protons on the fiber surface [labeled as group C] are also accelerated in the radial direction by this electric field, forming the fine ring

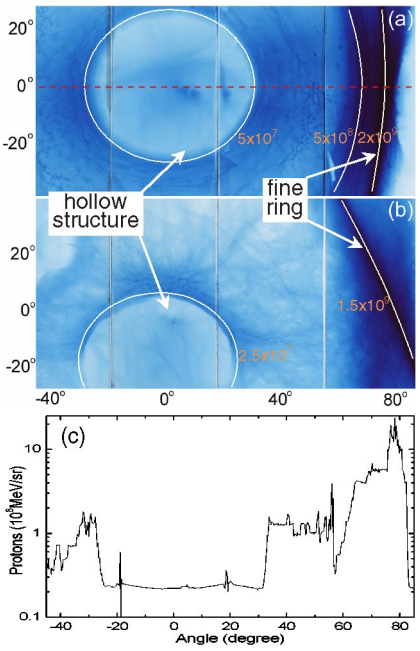

FIG. 2 (color online). Angular distributions of protons at approximately 6–8 MeV measured by RCFs, with laser beam at $(0°, 0°)$, from (a) the straight-fiber cone and (b) the tilted-fiber cone. The proton distribution along the red dashed line in (a) is shown in (c). The white curves in (a) and (b) show the contour lines of protons per solid angle number. The small dim spot close to the fiber axis in the hollow is from the escaped hot electrons.

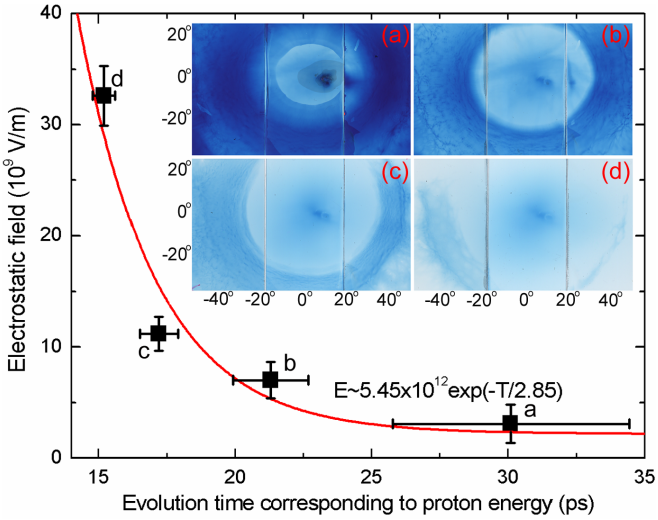

FIG. 3 (color online). The energy dependence of the proton angular distribution around the fiber axis in the straight-fiber cone and a corresponding fitting curve of the time evolution of the radial electric field. Dots on the curve correspond to the images with the same serial number. The hollow diameter increases when the proton energy changes from (a) 3–5.8 MeV, (b) 6–8 MeV, and (c) 9.2–10.9 MeV to (d) 11.8–13.1 MeV.

perpendicular to the fiber axis. Finally, the fiber expands in the radial direction at a high speed (proved by the experimental observation of optical and soft x-ray and extreme ultraviolet emissions [9,12,13]) due to the fast heating by the guided electrons. This expansion further spreads the electric field radially around the fiber. When protons in group A pass by the fiber, they experience the radial electric field and are thus deflected outwards, forming a hollow structure with no protons near the fiber axis. This expanding fiber plasma together with the proton deflection by the radial field can explain the significantly reduced number of protons per unit area observed here compared with that in the simple reentrant cone [11], in particular, for those with relatively low energies.

The energy dependence of the hollow diameter shown in Fig. 3 can also be explained by the transient radial electric field on the fiber surface. Initially this field keeps on increasing until a peak value is reached, due to the electron transport starting from the laser plasma interaction. It then decreases because of field diffusion processes such as TNSA and thermal expansion in the plasma fiber. The protons in group A suffer from a time-dependent deflection by this electric field while moving forward. A larger deflection is thus expected for those with higher energies because they are generated at earlier time from the disk and experience a relatively larger radial field on the fiber, resulting in a larger diameter in the hollow structure. This different deflection helps one to understand the time evolution of the radial electric field [see Fig. 3]. It is shown to decay exponentially within approximately 3 ps from a peak value of 5×10^{12} V/m. This is obtained by fitting the estimated electric field to the transition time of protons moving from one end of the fiber attached to the cone-disk tip to another. The electric field is estimated based on the proton energy and its deflection angle shown by the hollow diameter in the inset images of Fig. 3. The transition time is estimated based on the proton velocity and the fiber length (1 mm).

One of the possible advantages of this radial electric field is to transfer the radial momentum in the guided MeV electron beam to the accelerated protons, resulting in a better collimation (as small as a few degrees [9]) for the energetic electron beam. It is well known that the hot electrons generated in laser plasma interaction have a beaming angle as large as 40°. The radial electric field around the fiber can be thought of as being induced by the transverse momentum in the electron beam. Therefore part of the momentum is transferred from the electron beam to accelerate the protons on the fiber surface. An estimate based on the measured energy spectrum of the protons in the fine ring suggests that the total energy carried in this way by the protons between 0.5 and 20 MeV is approximately 17 mJ. On the other hand, the guided MeV electrons could have an energy of approximately 11 J, with assumption of an energy transfer of about 6% from the laser [9]. Consequently, the energy carried by the protons decreases the guided electron beaming angle by approximately 10°, considering approximately 5% of the energy transfer efficiency [4] from the transverse energy in the guided electrons to the accelerated protons in the fine ring. We assume here that both the transverse and longitudinal momenta in the electron beam have a Gaussian distribution and their temperature ratio decides the beam angle.

Two-dimensional PIC simulations were conducted to further clarify the physical mechanism associated with the proton angular distributions discussed above. Our code solves the relativistic equations of motion for particles and the Maxwell equations self-consistently [14]. A fiber plasma with the transverse and longitudinal dimensions $5\lambda \times 200\lambda$ at a few times the critical density is assembled either to a cone tip or a plane target in the simulations. A laser pulse with a focused diameter $\sim 20\lambda$ and a duration around 200 laser cycles is incident normally onto the target. The focused peak laser intensity is around 1.2×10^{19} W cm^{-2} at a wavelength of $\lambda = 1$ μm. For simplicity, only the results for the case of a fiber plasma attached to a plane target are given in the following, since we are mainly interested in the particle transport through the plasma fiber. A cone structure introduces additional proton acceleration normal to the cone wall only, as expected. Figures 4(a) and 4(b) shows snapshots of the transverse field, which is perpendicular to the plasma fiber axis. It is induced near the plasma fiber surface in vacuum for lack of the charge neutrality. Our simulation shows that the peak radial field can be as large as $\sim m\omega_0 c/e = 3.2 \times 10^{12}$ V/m at the predefined conditions for the laser and target. It decays and spreads with time as the laser interaction terminates and the energetic electrons propagate through the fiber. The electron spatial distribution [the left column of Fig. 4(c)] shows a collimated electron beam through the fiber, where a significant part of electrons moves inside the fiber and the remaining part is outside the fiber surface. Charge neutrality by the return current inside the fiber plasma results in zero electrostatic field there both in longitudinal and radial directions. This can be illustrated by the energetic proton distribution in the coordinate space [the right column of Fig. 4(c)], where no energetic proton is found inside the plasma fiber. Protons on the fiber surface are accelerated dominantly in the radial direction by the radial field, as shown in the momentum space in Fig. 4(d) (top panel). The angular distribution given in Fig. 4(e) shows that protons on the plasma fiber are emitted close to 90°, i.e., normal to the fiber surface [also see Fig. 4(d), top panel]. These protons are responsible for the fine ring in the proton angular distribution observed in our experiments. Besides, there are other proton emissions symmetrical about the fiber axis (0°). The temporal and spatial dependence of this proton emission shows a deflection by the radial electric field around the fiber surface. These protons are known to originate from the rear surface of

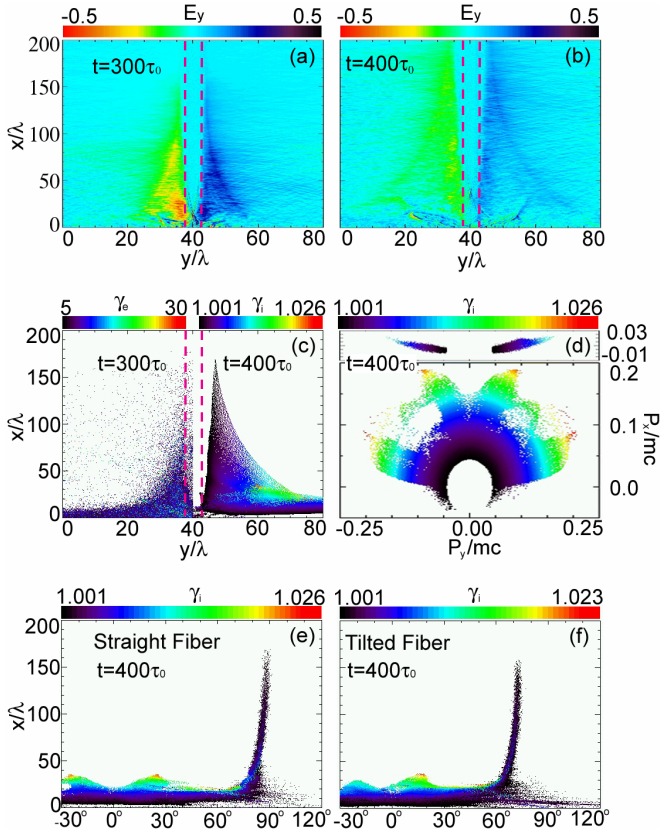

FIG. 4 (color online). Snapshots of 2D PIC simulations show the radial electric fields (normalized by $m\omega_0 c/e$) at the time of (a) $t = 300\tau_0$ and (b) $t = 400\tau_0$, (c) the spatial distributions of energetic electrons (left column) and protons (right column), (d) the momentum distribution of energetic protons along the fiber (top panel) and at the rear surface of the disk (bottom panel), and the energetic proton angular distributions in (e) the straight-fiber geometry and (f) the tilted-fiber geometry. The rear surface of the disk is located at $x/\lambda = 0$. The red dashed lines in (a)–(c) show the original fiber, which is directed at 0° as the incident laser pulse. λ is the laser wavelength, γ_e and γ_i are the relativistic factors of the electrons and protons, and τ_0 is the laser cycle.

the assembled plane target (i.e., group A) and are responsible for the hollow structure in the proton distribution [also see bottom panel of Fig. 4(d)]. As the fiber plasma is tilted by 15°, both proton emissions close to 0° and 90° change their directions to follow the fiber, as shown in Fig. 4(f), in agreement with our experiments.

In summary, we have reported an experimental study of the transient electrostatic fields and the related proton generation when MeV electrons are guided through the plasma fiber [9]. It is shown that the proton angular distribution with a hollow structure and an intense fine ring is produced via an induced radial electric field around the fiber. A time evolution of this electric field is deduced through the dependence of the hollow diameter on the proton energy, which is found to decay exponentially within approximately 3 ps from 5×10^{12} V/m.

We thank the technical staff at the Institute of Laser Engineering for their support in laser system operation, target fabrication, and data acquisition. G. R. K. thanks JSPS for supporting his visit. Z. M. S. was supported in part by the National High-Tech ICF committee and the National Natural Science Foundation of China (Grants No. 10425416 and No. 10335020).

*Current address: Department of Electrical and Computer Engineering, University of Alberta, Edmonton T6G 2V4, Canada.
Electronic address: zhenglinchen@hotmail.com
†Permanent address: Tata Institute of Fundamental Research, Mumbai, India.

[1] N. G. Basov *et al.*, J. Sov. Laser Res. **13**, 396 (1992); M. Tabak *et al.*, Phys. Plasmas **1**, 1626 (1994).
[2] T. E. Cowan *et al.*, Phys. Rev. Lett. **84**, 903 (2000); K. W. D. Ledingham *et al.*, Science **300**, 1107 (2003); E. Liang and K. Nishimura, Phys. Rev. Lett. **92**, 175005 (2004); F. N. Beg *et al.*, Phys. Rev. Lett. **92**, 095001 (2004).
[3] A. Modena *et al.*, Nature (London) **377**, 606 (1995); G. Malka *et al.*, Phys. Rev. Lett. **79**, 2053 (1997); E. P. Liang, S. C. Wilks, and M. Tabak, Phys. Rev. Lett. **81**, 4887 (1998); M. Hegelich *et al.*, Phys. Rev. Lett. **89**, 085002 (2002); T. E. Cowan *et al.*, Phys. Rev. Lett. **92**, 204801 (2004); S. P. D. Mangles *et al.*, Nature (London) **431**, 535 (2004); C. G. R. Geddes *et al.*, Nature (London) **431**, 538 (2004); J. Faure *et al.*, Nature (London) **431**, 541 (2004).
[4] P. A. Norreys *et al.*, Phys. Plasmas **7**, 3721 (2000); R. Kodama *et al.*, Nature (London) **412**, 798 (2001); M. H. Key, Nature (London) **412**, 775 (2001); R. Kodama *et al.*, Nature (London) **418**, 933 (2002).
[5] Y. Glinec *et al.*, Phys. Rev. Lett. **94**, 025003 (2005).
[6] E. L. Clark *et al.*, Phys. Rev. Lett. **84**, 670 (2000); R. A. Snavely *et al.*, Phys. Rev. Lett. **85**, 2945 (2000).
[7] S. C. Wilks *et al.*, Phys. Plasmas **8**, 542 (2001); P. K. Patel *et al.*, Phys. Rev. Lett. **91**, 125004 (2003).
[8] M. Roth *et al.*, Phys. Rev. Lett. **86**, 436 (2001); M. Borghesi *et al.*, Phys. Plasmas **9**, 2214 (2002); A. J. MacKinnon *et al.*, Rev. Sci. Instrum. **75**, 3531 (2004).
[9] R. Kodama *et al.*, Nature (London) **432**, 1005 (2004).
[10] Y. Kitagawa *et al.*, IEEE J. Quantum Electron. **40**, 281 (2004).
[11] Z. L. Chen *et al.*, Phys. Rev. E **71**, 036403 (2005).
[12] R. Kodama *et al.*, Rev. Sci. Instrum. **70**, 625 (1999).
[13] Experiment at CLF, Rutherford Appleton Laboratory, by R. A. Snavely, LLNL (2004).
[14] Z. M. Sheng *et al.*, Phys. Rev. E **69**, 025401(R) (2004).